

Behavior of Geogrid-Sand Interface in Direct Shear Mode

Chia-Nan Liu¹; Jorge G. Zornberg, M.ASCE²; Tsong-Chia Chen³; Yu-Hsien Ho⁴; and Bo-Hung Lin⁵

Abstract: The contribution of transverse ribs to the soil-geogrids interaction under pullout mode has been well documented. However, the contribution of transverse ribs to the soil-geogrid interaction under direct shear mode is, at best, unclear. Consequently, this paper presents the results of a comprehensive direct shear testing program aimed at evaluating the contribution of transverse ribs to the interface shear. The direct shear tests involved Ottawa sand and several polyester geogrids with a variety of material tensile strength, percent open area, and aperture pattern. The test results show that the shear strength of sand-geogrid interfaces under direct shear mode is significantly higher than that of sand-geotextile interfaces. Analysis of shear displacement-strength response of the interfaces indicates that, in addition to interface shear components due to sand-rib friction and sand-sand shear at the location of the openings, the transverse ribs provide additional contribution to the overall sand-geogrid interface resistance. Specifically, analysis of the results reveals that the transverse ribs of the geogrid used in this study provide approximately 10% of interface shear resistance. This contribution is positively correlated with the tensile strength and the stiffness of geogrid ribs, but is negatively correlated with the percent open area of the geogrid. A simple model is proposed to quantify the contribution of transverse ribs to the interface shear strength under direct shear mode.

DOI: 10.1061/(ASCE)GT.1943-5606.0000150

CE Database subject headings: Shear tests; Geogrids; Geosynthetics; Interfaces; Sand, soil type.

Introduction

The contribution of transverse ribs to the soil-geogrid interaction has been quantified in the technical literature by passive resistance mechanisms using pullout tests (e.g., Koerner et al. 1989; Jewell 1990; Bergado et al. 1993; Sugimoto et al. 2001; Palmeira 2004; Teixeira et al. 2007). The pullout failure mode plays a significant role in the design of geogrid-reinforced soil structures and it has been used for evaluation of internal stability of reinforced soil walls. However, the design of geogrid-reinforced soil structures should also assess the response of the structure for the case of failure surfaces that may develop along the soil-geogrid interface (i.e., direct shear failure mode). The contribution, if any, of transverse ribs to the soil-geogrid interaction under direct shear mode has not been properly quantified. Quantification of this contribution is the focus of this investigation. Proper representation of the soil-geosynthetic interfaces under direct shear mode is also important for numerical simulation of the deformation response of retaining structures (e.g., Hatami and Bathurst 2006). The shear strength of soil-geogrid interfaces has been investigated

using direct shear tests by Jarret and Bathurst (1985), Cancelli et al. (1992), Bauer and Zhao (1993), Cazzuffi et al. (1993), Bakeer et al. (1998), and Abu-Farsakh and Coronel (2006). While previous studies have provided good insight into the interface shear strength along soil-geogrid interfaces, the actual passive resistance contribution of transverse ribs has not been clearly identified.

In the case of geomembranes and geotextiles, the interface shear resistance against soil results solely from the shear resistance between the geosynthetic surface against soil particles because soil particles are not interlocked with openings. However, the interaction mechanisms under direct shear mode between soil and geogrids are more complex than those between soil and sheet geosynthetics. Geogrids are characterized by a combination of longitudinal and transverse ribs. Therefore, the interactions between soil and geogrid may include the following mechanisms: (1) shear resistance between soil and the surface of the geosynthetic (the ribs, in the case of geogrids); (2) internal shear resistance of the soil (in the opening area); and (3) passive resistance of the transverse ribs. The mechanisms (1) and (2) have been quantified by researchers such as Alfaro et al. (1995) and Tatlisoz et al. (1998). On the other hand, while the contribution of geogrid transverse ribs has been recognized to provide significant passive resistance for the case of interaction under pullout mode (e.g., Jewell 1990; Bergado et al. 1993; Palmeira 2004), the contribution of transverse ribs under direct shear mode is a subject of controversy. For example, Lopez (2002) reported that the contribution of the passive resistance induced by the transverse ribs of geogrids is almost negligible under direct shear mode. On the other hand, Bergado et al. (1993) stated that the apertures of geogrids provided significant passive resistance in a series of direct shear tests on high-density polyethylene (HDPE) geogrid-soil interfaces. Consequently, this study aims at clarifying the contribution of geogrid transverse ribs to the shear strength of geogrid-soil interfaces.

The soil-geogrid interaction under direct shear mode may govern the stability of geosynthetic reinforced soil structures. How-

¹Professor, Dept. of Civil Engineering, National Chi-Nan Univ., Nantou 545, Taiwan (corresponding author). E-mail: cnliu@nccu.edu.tw

²Fluor Centennial Associate Professor, Dept. of Civil, Architectural, and Environmental Engineering, Univ. of Texas at Austin, Austin, TX 78712.

³Former Graduate Student, Dept. of Civil Engineering, National Chi-Nan Univ., Nantou 545, Taiwan.

⁴Graduate Student, Dept. of Civil Engineering, National Chi-Nan Univ., Nantou 545, Taiwan.

⁵Graduate Student, Dept. of Civil Engineering, National Chi-Nan Univ., Nantou 545, Taiwan.

Note. This manuscript was submitted on December 5, 2007; approved on May 20, 2009; published online on November 13, 2009. Discussion period open until May 1, 2010; separate discussions must be submitted for individual papers. This paper is part of the *Journal of Geotechnical and Geoenvironmental Engineering*, Vol. 135, No. 12, December 1, 2009. ©ASCE, ISSN 1090-0241/2009/12-1863-1871/\$25.00.

Table 1. Geosynthetic Geometric Characteristics

Material	Aperture length l (mm)	Aperture Width w (mm)	Longitudinal rib width l_w (mm)	Transverse rib width t_w (mm)	Percent open area (%)	Stiffness of geogrid ribs (kN/m)	Ultimate tensile strength (kN/m)	
							Machine direction	Cross-machine direction
GT	—	—	—	—	—	—	100	50
GG1	26.5	22.1	6.6	4.7	65	20.3	60	30
GG2	26.3	21.6	6.9	4.6	64	23.5	100	30
GG3	26.6	18.5	10.1	4.6	55	49.8	200	40
GG4	7	7	2.5	3.2	49	22.2	100	100
GG5	36.9	17.3	15	1.2	46	48.9	200	40
GG6	17.2	7	2.5	3.2	61	19.8	100	50
GG7	17.2	16.5	2.5	3.2	72	14.5	50	50
GG8	57.8	18.5	10.1	4.6	60	42.4	200	20
GG9	436	7	2.5	3.2	73	17.1	100	0
GG1T	22.1	26.5	4.7	6.6	65	10.8	30	60
GG2T	21.6	26.3	4.6	6.9	64	12.6	30	100
GG3T	18.5	26.6	4.6	10.1	55	15.3	40	200

ever, most studies on soil-geogrid interfaces have focused on reporting the overall interface shear strength, with little insight into identifying the different components contributing to the interface shear resistance. In order to evaluate the relative contribution of the three aforementioned mechanisms to the overall shear resistance of soil-geogrid interfaces, a series of large-scale direct shear tests was conducted as part of this study. The test results obtained from this experimental testing program allow quantifying these various components in order to further the understanding of the soil-geogrid interface shear properties.

Material Used in the Experimental Programs

Ottawa sand was used in the direct shear tests conducted throughout this study. This sand, which classifies as SP according to the Unified Soil Classification System, was used at a water content of approximately 4.5%, which corresponds to air-dried conditions. The dry unit weight of the compacted soil specimens was 16.7 kN/m^3 , which corresponds to a relative density (D_r) of 80%. Six geosynthetics, including a woven geotextile and five geogrids, were used in this study. The six geosynthetics are denoted as GT, GG1, GG2, GG3, GG4, and GG5, respectively. For consistency in the analysis of the results presented as part of this study, the selected geosynthetics were manufactured using polyester (PET) yarns coated with PVC. The geogrids are commercially available products, produced by a single manufacturer, while the PVC-coated geotextile was specially manufactured by the same provider for the purposes of this study. The physical characteristics of these geosynthetics are listed in Table 1. These characteristics include the size of apertures, width of ribs, percent open area (i.e., the ratio of overall aperture area to geogrid area), stiffness of geogrid at 2% strain, and ultimate tensile strength. As will be discussed, geogrids GG6, GG7, GG8, and GG9 were obtained by removing ribs to other geogrid products.

Test Equipment and Procedures

A large-scale direct shear device was used in this study, which consisted of a rigid steel base constructed with U-shaped steel

beams. The length, width, and thickness of the upper and lower shear boxes were 450, 450, and 130 mm, respectively. The shearing area was 0.2025 m^2 . As indicated in Federal Highway Administration (2001), because interaction behavior between geogrids and soils is complex, a large testing area should be used to characterize interfaces involving geogrids. The length and width of the shear box exceeded 15 times the maximum size of the apertures of the geogrids used in this study. The movement of the lower shear box in the horizontal direction was controlled by a set of gears mobilized by an electric motor. The vertical loading system involved a hydraulic jack acting against a rigid reaction frame that applied the normal load on a rigid plate placed on top of the upper shear box. This loading system allowed good control of the normal stress during testing, even when the soil showed significant volumetric changes (dilatancy or contraction) during shearing. The variation of normal load during testing was below 2%, which satisfies the ASTM D5321 requirement (ASTM 2002). The system was capable of applying vertical and shear forces of up to 10,000 kN. Fig. 1 shows a frontal view of the large-scale direct shear device used in this study. The applied vertical force,

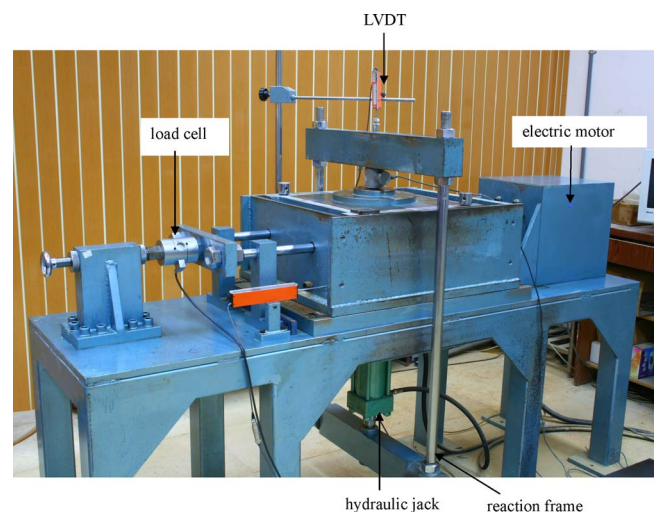


Fig. 1. View of large-scale direct shear apparatus

vertical displacement, applied shear force, and horizontal displacement of lower shear box were recorded throughout the tests. These data were collected using two load cells and two linear variable displacement transformers (LVDTs). The capacity of the load cells was 10,000 kN while the range of the vertical and horizontal LVDTs were 50 and 100 mm, respectively.

The Ottawa sand used in the large-scale direct shear testing program was placed at the target unit weight within the lower shear box. The sand was compacted in three layers using an electric vibrator. The geosynthetic specimen was then positioned on top of the lower shear box and subsequently clamped on the front edge of the lower shear box using seven aligned bolts and a steel clamping block. The direct shear tests were conducted using normal loads of 8.5, 18.5, and 38.0 kN, which correspond to nominal normal stresses of 42, 92, and 187 kPa, respectively. The testing procedure involved applying the normal load and monitoring the vertical displacement of the specimens during the test. The shear load was only applied after the vertical displacement had reached equilibrium after applying the vertical load. Consistent with ASTM D5321, a shear displacement rate of 1 mm/min was used during testing. Excess pore water pressures generated at the interface of air-dried Ottawa sand and geogrid, if any, would dissipate at this displacement rate. The tests were terminated when the shear displacement reached approximately 69 mm (i.e., about 15% shear strain, which corresponds to the maximum travel allowed in the equipment). The maximum shear strength obtained during the shear process was recorded as the peak shear strength.

Scope of the Testing Program

A set of large-scale direct shear tests were initially performed with the objective of quantifying the internal shear strength of Ottawa sand and therefore the contribution of shear resistance through the geogrid openings. Subsequently, the interface shear strength between the woven geotextile and the sand was determined with the objective of quantifying the component of shear resistance that develops between the sand and the surface of the geogrids ribs. These components were used as reference values in the analysis of subsequent tests conducted to evaluate the sand-geogrid interface shear strength. Of particular interest was the study of the effect of longitudinal ribs, transverse ribs, and percent open area on the shear strength of sand-geogrid interface. For the purpose of increasing the range of geometric characteristics of the geogrids, a fraction of longitudinal and transverse ribs of geogrids GG3 and GG4 was removed in order to obtain specimens with larger percent open area. Specifically, GG6 corresponds to the geogrid in which half of the transverse ribs of geogrid GG4 were removed, GG7 corresponds to the geogrid in which half of the transverse and longitudinal ribs of geogrid GG4 were removed, GG8 corresponds to the geogrid in which half of the transverse ribs of geogrid GG3 were removed, and GG9 corresponds to the geogrid in which all the transverse ribs of geogrid GG4 were removed. Fig. 2 shows a view of the various geosynthetics used in this study. Direct shear tests were also conducted using GG1, GG2, and GG3 specimens tested in the cross-machine direction. The transposed arrangements allowed evaluation of reinforcements with different longitudinal and transverse tensile strength values but with the same percent open area. The geogrids tested in the cross-machine direction are denoted as GG1T, GG2T, and GG3T, respectively.

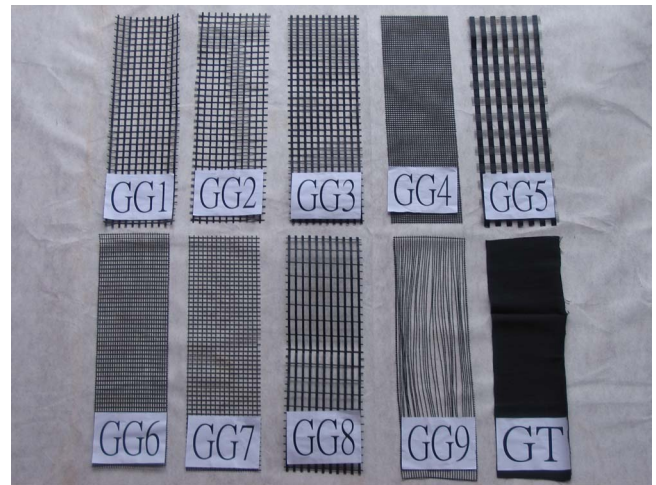


Fig. 2. Geosynthetic specimens used in this investigation

Direct Shear Test Results

The shear stress versus shear displacement curves obtained from the direct shear tests conducted on sand, on sand-geotextile interfaces, and on sand-GG3 interfaces are shown in Fig. 3. The sand internal and sand-geotextile interfaces show a reasonably well-defined peak shear strength, which is reached at comparatively small shear displacements (usually below 20 mm). The shear stress at any shear displacement value (and in particular the peak shear strength) obtained from direct shear tests on sand is consistently higher than that obtained from direct shear tests on the sand-geotextile interface. On the other hand, the shear stress-displacement behavior of the sand-geogrid interface shows a different pattern. Specifically, a “yield” shear stress with a value slightly higher than the peak shear strength of the sand-geotextile interface develops at a shear displacement similar to the shear displacement at peak of the sand-geotextile interface (below

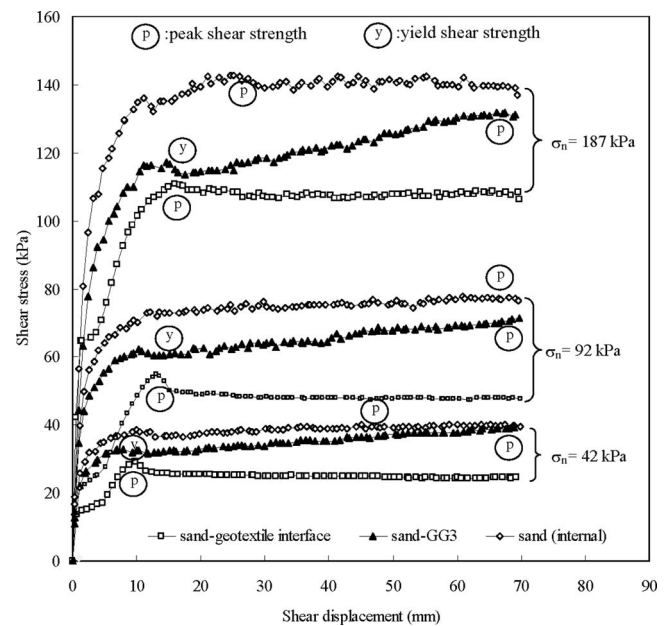


Fig. 3. Shear stress-displacement behavior of Ottawa sand, sand-geotextile interface, and sand-GG3 interface

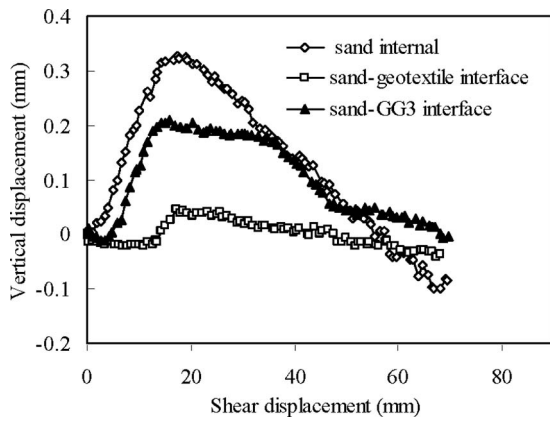


Fig. 4. Vertical displacement versus shear displacement results for direct shear tests of Ottawa sand (internal), sand-geotextile interface, and sand-GG3 interface

20 mm). The shear stress of the sand-geogrid interface continues to increase beyond this yield shear stress, approaching to the peak shear strength of the sand for comparatively large shear displacement values. That is, the sand-geogrid response is bound between the sand-geotextile and sand shear stress-displacement curves within the range of shear displacement used in this study (69 mm). It should be noted that the geogrids and woven geotextiles used in this testing program have been manufactured using the same material (PVC-coated PET yarns). The shear displacement at peak for the sand-geogrid interface is always larger than the shear displacement at peak for the Ottawa sand and for the sand-geotextile interfaces. These results suggest that the internal shear resistance of the sand particles (across the openings, in the case of the geogrid) and the shear resistance between sand and the surface of the geosynthetics (surface of the ribs, in the case of the geogrid) contribute to the overall direct shear resistance at small displacements. On the other hand, the passive resistance developed by transverse ribs of the geogrid appears to contribute to the overall shear resistance at comparatively larger displacements.

The vertical displacement versus shear displacement curve obtained from the direct shear test on the sand-GG3 interface is shown in Fig. 4. As shown in the figure, the geogrid-sand interface undergoes an initial vertical contraction for small values of shear displacement. Subsequently, the specimen exhibits dilatancy for larger values of shear displacement. A comparison with the vertical deformation behavior of pure sand, also shown in the figure, reveals that the geogrid-sand interface experiences comparatively smaller vertical displacement during shearing. It is interesting to note that the maximum dilatancy of the sand-GG3 occurs at the shear displacement that corresponds to the yield shear stress rather than at the shear displacement that corresponds to the peak shear strength of the interface.

It is recognized that the ultimate shear strength that can be achieved by the soil-geogrid interfaces may exceed the failure criterion adopted in this study (i.e., shear at a maximum shear displacement of 69 mm). Consequently, it is important to highlight the relevance of the yield stress observed in the shear stress-displacement behavior of the soil-geogrid interfaces. Its relevance stems from two main aspects. First, the yield stress appears to correspond to the maximum contribution to interface shear provided by the aforementioned mechanisms (1) and (2). Second, the yield stress takes place at a shear displacement that is consistent in magnitude with the shear displacement at peak of the sand-

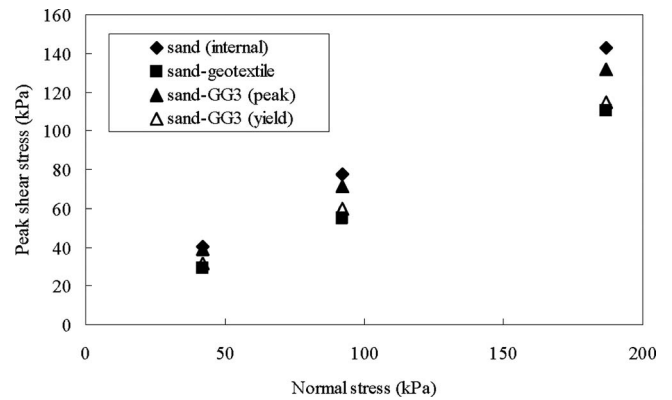


Fig. 5. Peak shear strength of Ottawa sand (internal), sand-geotextile interface, and sand-GG3 interface

geotextile interface and of the pure sand. Consequently, comparison of the yield stress of sand-geogrid interfaces with the peak shear strength of sand-geotextile interfaces provides insight into the shear stresses at an equivalent level of displacement. The peak and yield shear strength of sand-GG3 interface is presented in Fig. 5. A linear shear strength envelope fitting the experimental results would define a cohesion intercept. This intercept may be induced by negative pore water pressure due to small water content in sand, or is probably due to nonlinearity of the shear strength envelope. The conventional Mohr-Coulomb failure criterion is not used to fit the shear strength data. The peak internal shear strength of Ottawa sand (τ_{sand}) at each normal stress used in the testing program was adopted as a baseline shear strength value. The shear strength values of sand-geosynthetic interfaces ($\tau_{sand-geosynthetic}$) were normalized using the baseline values at the corresponding stress level ($\sigma_n = 42, 92, \text{ and } 187 \text{ kPa}$). The normalized value is identified as the interface shear strength coefficient, α , in this study. Similar relationships have been identified in the literature as the “bond coefficient” (Bergado et al. 1993), and the “interface efficiency” (Tatlisoz et al. 1998). That is

$$\alpha = \tau_{sand-geosynthetic} / \tau_{sand} \quad (1)$$

The interface shear strength coefficients of different sand-geogrid interfaces are shown in Fig. 6. Consistent with the test results

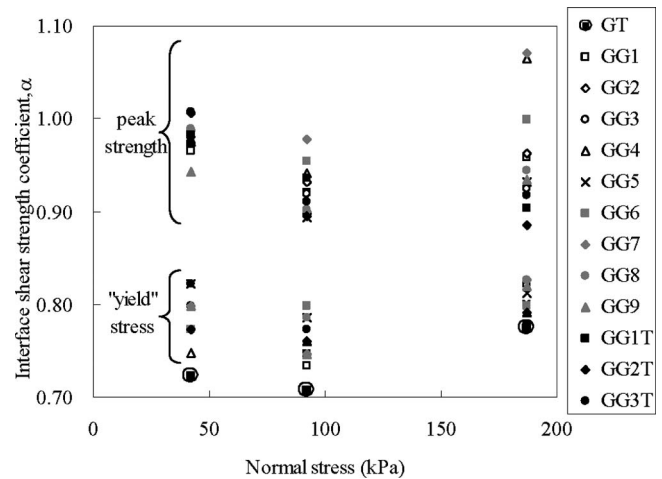


Fig. 6. Interface shear strength coefficient, α , for the different sand-geosynthetic interfaces

Table 2. Direct Shear Test Results

Interface	Normal stress=42 kPa			Normal stress=92 kPa			Normal stress=187 kPa						
	τ_{\max} (kPa)	α	β	τ_{\max} (kPa)	α	β	τ_{\max} (kPa)	α	β	μ_{α}	σ_{α}	μ_{β}	σ_{β}
Sand	40.1	1.00	—	77.6	1.00	—	142.7	1.00	—	1.00	0	—	—
Sand-GT	29.1	0.72	—	55.0	0.71	—	110.8	0.78	—	0.74	0.035	—	—
Sand-GG1	38.7	0.96	0.06	71.5	0.92	0.02	136.7	0.96	0.04	0.95	0.024	0.04	0.020
Sand-GG2	40.4	1.01	0.11	72.3	0.93	0.04	137.4	0.96	0.04	0.97	0.038	0.06	0.038
Sand-GG3	39.1	0.97	0.10	71.4	0.92	0.05	131.8	0.92	0.02	0.94	0.031	0.06	0.038
Sand-GG4	39.1	0.98	0.12	73.1	0.94	0.09	151.9	1.06	0.18	0.99	0.064	0.13	0.046
Sand-GG5	39.2	0.98	0.13	69.4	0.89	0.05	133.0	0.93	0.05	0.93	0.041	0.08	0.042
Sand-GG6	39.6	0.99	0.09	74.1	0.95	0.07	142.6	1.00	0.09	0.98	0.023	0.08	0.013
Sand-GG7	39.6	0.99	0.07	75.9	0.98	0.06	152.8	1.07	0.13	1.01	0.051	0.09	0.041
Sand-GG8	39.7	0.99	0.10	70.0	0.90	0.02	134.8	0.94	0.03	0.95	0.043	0.05	0.043
Sand-GG9	37.8	0.94	0.02	70.2	0.90	-0.02	133.3	0.93	-0.01	0.93	0.020	0.00	0.017
Sand-GG1T	39.4	0.98	0.08	72.7	0.94	0.04	129.0	0.90	-0.02	0.94	0.039	0.03	0.048
Sand-GG2T	39.1	0.97	0.07	69.5	0.90	0.00	126.4	0.89	-0.03	0.92	0.049	0.01	0.055
Sand-GG3T	40.4	1.01	0.13	70.7	0.91	0.04	131.0	0.92	0.02	0.95	0.054	0.06	0.059

presented in Fig. 5 for one set of interface shear tests, Fig. 6 shows that the sand-geotextile interface strength is significantly lower than the shear strength of the sand. Since the size of apertures in the woven geotextile is too small to allow for direct contact between sand particles, the shear resistance of this interface can be attributed to a single mechanism, that is, shear between the geosynthetic surface and the sand particles. The interface shear strength coefficient (α) of sand-geotextile ranges from 0.7 to 0.8. Similar values have been reported in technical literatures (e.g., Martin et al. 1984). That is, the shear strength of the soil-geotextile interface is lower than the shear strength of the soil. The yield stress of the various sand-geogrid interfaces are also shown in Fig. 6. As shown in this figure, and consistent with the remarks made previously for the case of GG3 test results, the yield stress of sand-geogrid interfaces is similar to the peak strength of the sand-geotextile interface, while the “peak” strength of sand-geogrid interface is approaching the peak shear strength of the sand ($\alpha=1$).

The interface shear strength coefficient (α) values for the different sand-geogrid interfaces are listed in Table 2. It can be observed that the interface shear strength coefficient (α) of sand-geogrid interfaces generally ranges from 0.9 to 1, although some values are as high as 1.07. The mean interface shear strength coefficient of each sand-geogrid interface was calculated as the average of the three values obtained at each normal stresses. For the sand-geogrid interfaces tested in this study, the mean interface shear strength coefficient ranges from 0.92 to 1.01, with standard deviation values ranging from 0.02 to 0.06.

The α values obtained in this study are generally consistent with those reported in previous investigations. Cancelli et al. (1992) reported interface shear strength coefficients ranging from 1.04 to 1.12 for interfaces between HDPE and polypropylene (PP) geogrids against sand, Cazzuffi et al. (1993) reported interface shear strength coefficient of 0.97 for sand-HDPE geogrid interface, while Bakeer et al. (1998) reported interface shear strength coefficient of 0.92 for lightweight aggregate-HDPE geogrid interface. Abu-Farsakh and Coronel (2006) found interface shear strength coefficients for sand-PET geogrid interface ranging from 0.90 to 1.05 for various conditions of soil density and water content.

The interface shear strength of sand-geogrid interface obtained in this study is higher than that of sand-geotextile interface. The

higher interface shear strength is attributed to the effect of geogrid apertures and transverse ribs, which provide passive resistance even under direct shear mode. The pattern of shear stress-displacement of the sand-geogrid interface shown in Fig. 3 provides evidence that the additional strength is developed from passive resistance induced by the transverse ribs. This is because passive resistance mechanisms develop at comparatively large shear displacements. On the other hand, mechanisms involving shear resistance between sand and the surface of the geosynthetic (see pattern of sand-geotextile interface) or internal shear resistance of the sand (see pattern of internal sand shear strength) develop at comparatively small shear displacements.

The shear strength of sand-geogrid interfaces under direct shear mode has been usually attributed to shear resistance between sand and the surface of the geosynthetic (the ribs, in the case of geogrids), and internal shear resistance of the sand (in the geogrid openings). A conventional expression (e.g., Bergado et al. 1993) proposed to predict the shear strength in a sand-geogrid interface mobilized under direct shear mode is

$$\tau_{\text{sand-geogrid}} = \sigma_n \times [(1 - \rho)\tan \delta + \rho \tan \Phi_{ds}] \quad (2)$$

where ρ =percent open area of geogrid; δ =interface friction angle between sand and geosynthetic; and Φ_{ds} =internal friction angle of sand obtained from direct shear tests. Eq. (2) can be rearranged as

$$\tau_{\text{sand-geogrid}} = (1 - \rho)\tau_{\text{sand-geosynthetic}} + \rho \tan \tau_{\text{sand}} \quad (3)$$

That is, the interface shear strength of sand against geogrid is estimated by adding the shear strength of sand and the shear strength of the sand-geosynthetic interface, weighted respectively by the percent open area and the geosynthetic area ratio. The geosynthetic area ratio, which equals $(1 - \rho)$, is the ratio of the area of ribs (longitudinal and transverse) to the total geogrid area. Information about the percent open area and the geosynthetic area ratio for the materials used in this study is shown in Table 1, while the shear strength of sand (τ_{sand}) is shown in Table 2. In addition, the shear resistance between sand and the surface of the geosynthetic ($\tau_{\text{sand-geosynthetic}}$) was defined in this study using the results reported in Table 2 from direct shear tests conducted on sand-geosynthetic interfaces. These measured values were used with Eq. (3) to predict the shear strength of each sand-geogrid interface, accounting only for the shear resistance between sand

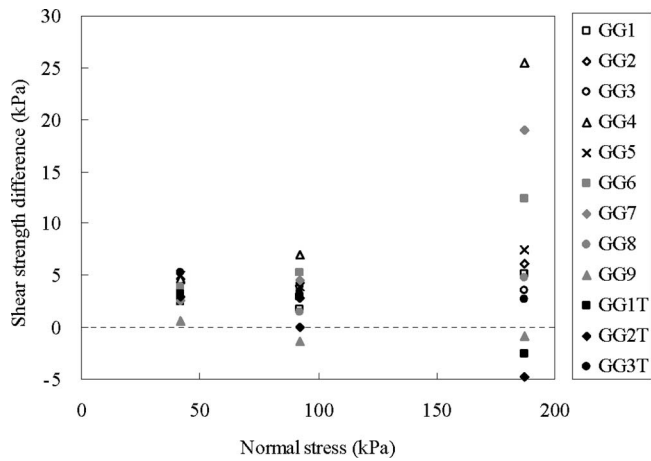


Fig. 7. Deviation of measured shear strength from value predicted by Eq. (3)

and the surface of the geogrid ribs, and the internal shear resistance of the sand [mechanisms (i) and (ii)]. The differences between the measured and predicted shear strength are shown in Fig. 7, which indicates that the shear strength predicted by Eq. (3) does not compare well with the measured values. In most cases, the magnitude of the predicted shear strength is smaller than the measured value. Also, the peak shear strength of sand-geotextile interfaces develops at smaller shear displacements than the peak shear strength of sand-geogrid interfaces. Consequently, an additional mechanism should be contributing to the shear resistance of sand-geogrid interfaces at comparatively large shear displacements. These test results provide evidence that the passive resistance induced by transverse ribs [i.e., mechanism (3)] provides an additional sand-geogrid interface shear strength under direct shear mode.

Passive Resistance Contribution to Sand-Geogrid Interface Shear Strength

Inspection of the shear stress-displacement behavior of sand-geogrid interfaces (Fig. 4) and evaluation of the difference between measured and predicted interface shear strength when considering only mechanisms (1) and (2) provided evidence that passive resistance (mechanism 3) also contributes to the shear strength of sand-geogrid interfaces. A parameter is proposed to quantify the passive resistance contribution to the overall shear strength of sand-geogrid interfaces. Specifically, the passive resistance contribution ratio, β , is defined as

$$\beta = [\tau_{\text{sand-geogrid}} - (1 - \rho)\tau_{\text{sand-geotextile}} - \rho \tan \tau_{\text{sand}}] / \tau_{\text{sand-geogrid}} \quad (4)$$

That is, the passive resistance contribution is quantified as the difference between the measured overall direct shear strength and the pure shear resistance [mechanisms (1) and (2)]. The parameter β is the ratio between the passive resistance contribution and the overall direct shear strength.

The passive resistance contribution ratio (β) of different sand-geogrid interfaces are listed in Table 2. The results show that most of the β values of sand-geogrid interface range from 0 to 0.1, although some cases β is as high as 0.18. Of particular interest is the passive resistance contribution ratio (β) of test GG9, as all transverse ribs were removed. The β values obtained for test GG9

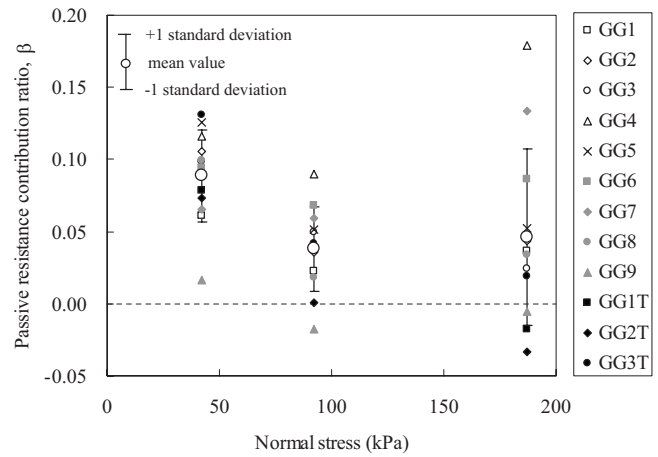


Fig. 8. Passive resistance contribution ratio, β , for different sand-geogrid interfaces

are essentially negligible (0.02, -0.02 , and -0.01 for normal stress of 42, 92, and 187 kPa, respectively). These results provide evidence that transverse ribs provide a passive resistance contribution under direct shear mode.

The passive resistance contribution ratio, β , for different sand-geogrid interfaces are shown in Fig. 8. The average and standard deviation of β values for different normal stress level are also shown in the figure. The results show that the average β value is largest ($\beta=0.09$) for a normal stress of 42 kPa, indicating that the passive resistance contribution is more significant at low stress levels. The passive resistance contribution ratio is similar for normal stress values of 92 and 187 kPa (approximately 0.05). However, the variability in β value increases with increasing normal stress levels.

The mean passive resistance contribution ratio (β) of each sand-geogrid interface was calculated by averaging the three values obtained for tests conducted at different normal stresses. Statistical data of the β value for different sand-geogrid interfaces are listed in Table 2. The average β values range from 0 to 0.13, with standard deviation values ranging from approximately 0.01 to 0.05. It is noted that β values range from 0.04 to 0.13 for commercially available geogrid products (GG1 to GG5). These results indicate that the passive resistance contribution is relevant under direct shear mode.

Two limitations are noted in the evaluation of the passive resistance contribution by Eq. (4). First, the shear stress of the sand-geogrid interface appears to continue to increase beyond the maximum displacement of 69 mm that corresponds to the maximum travel of the equipment used in this study. Consequently, the passive resistance contributed by geogrid ribs may indeed be higher than that reported in Table 2. Second, it should be noted that the calculated β values become negative in some cases. Possible explanation for these results is provided by Palmeira and Milligan (1989) and Milligan et al. (1990) who reported that passive resistance mobilization in pullout tests is reduced by the interface shear mobilization between soil and transverse ribs (and to a certain extent between soil and longitudinal ribs). This observation was confirmed by Teixeira et al. (2007) who conducted a series of pullout tests on individual longitudinal and transverse geogrid ribs. They measured a localized reduction in normal stresses in the vicinity of the longitudinal ribs for the case of pullout tests. A similar localized reduction in normal stresses may occur in the vicinity of longitudinal ribs tested under direct shear

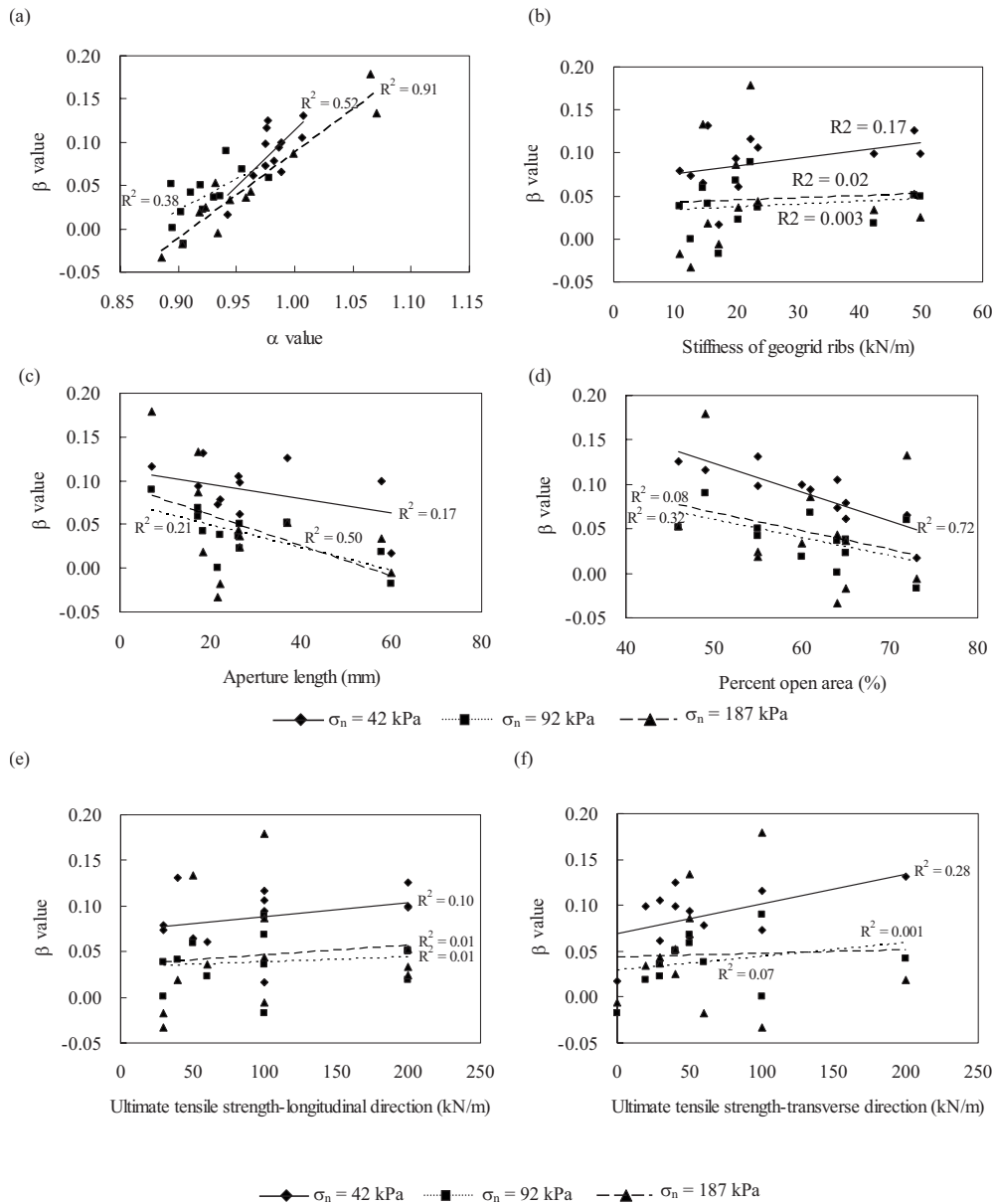


Fig. 9. Correlation of the passive resistance contribution ratio, β , with different parameters: (a) interface coefficient; (b) geogrid stiffness; (c) aperture length; (d) percent open area; (e) ultimate tensile strength in the longitudinal direction; and (f) ultimate tensile strength in the transverse direction

mode. It should be noted that a normal stress reduction is not expected for sand-geotextile interfaces because of the planar nature of geotextiles. Therefore, the use of sand-geotextile direct shear test results as shear resistance between sand and the surface of the ribs ($\tau_{\text{sand-geotextile}}$) in Eq. (4) may overestimate the shear resistance between sand and the surface of the geogrid ribs. Nonetheless, the contribution of transverse ribs to interface shear strength, as quantified by Eq. (4), provides a systematic approach to calculate the passive resistance contributed by geogrid ribs.

Factors Affecting the Passive Resistance Contribution

Fig. 9 summarizes the results of a parametric evaluation conducted to quantify the sensitivity of the passive resistance contribution ratio (β) to other relevant geogrid parameters. Trend lines

are shown for each normal stress ($\sigma_n=42, 92,$ and 187 kPa) to illustrate the effect of confinement on the passive resistance contribution. Steep trend lines indicate parameters with a significant effect on β while flat trend lines indicate a negligible effect. The coefficient of determination (R^2), in which R is the correlation coefficient, for each trend line is also shown in the figures. A small value of R^2 denotes comparatively low correlation with the selected parameter.

Fig. 9(a) shows that the passive resistance contribution ratio (β) is positively correlated with the interface shear strength coefficient (α). An increasing value of β with increasing α value (ratio of $\tau_{\text{sand-geogrid}}$ to the internal shear strength of sand) suggests that the sand-geogrid interface shear strength increases beyond the sand-geotextile values and are due to the passive contribution of transverse ribs. Fig. 9(b) shows the correlation of β with stiffness of geogrid measured at 2% strain. Fig. 9(c) shows that the passive resistance contribution decreases with increasing aperture

length. Consequently, the magnitude of passive resistance contribution is positively correlated to the number of transverse ribs. Fig. 9(d) shows that the passive resistance contribution decreases with increasing percent open area. Figs. 9(e and f) show the effect of the tensile strength of longitudinal and transversal ribs on the β value. Previous studies, conducted using large-scale direct shear tests on sand-geogrid interfaces, have reported that the tensile strength of HDPE and PP geogrids has little effect on interface shear strength (e.g., Cancelli et al. 1992). However, the test results obtained in this study indicate that increasing tensile strength of PET geogrids leads to higher passive resistance contribution. Although these correlations are not strong, similar trends were observed in both the machines and cross-machine directions.

Conclusions

A series of large-scale direct shear tests was conducted to evaluate the sand-geogrid interface shear strength using Ottawa sand and a variety of geosynthetics. Particular emphasis was placed on quantifying the contribution of passive resistance mechanisms to the overall shear strength of sand-geogrid interfaces. The main conclusions that can be drawn from this investigation are as follows:

- In addition to the shear resistance components (sand internal and sand-geogrid rib interfaces), the passive resistance induced by transverse ribs provides an additional contribution to the shear strength of sand-geogrid interfaces under direct shear mode.
 - The passive resistance contribution under direct shear mode takes place at shear displacement values that are comparatively large (i.e., larger than the shear displacement at peak of the soil). Consequently, a soil-geosynthetic system can rely on increased interface shear strength (beyond that induced by internal shear mechanisms) but only after developing comparatively large shear displacements.
 - The shear stress-displacement behavior of sand-geogrid interfaces shows a different pattern from that of the sand-geotextile and sand-sand interfaces. A yield shear stress with a value slightly higher than the peak shear strength of the sand-geotextile interface is observed at a shear displacement value similar to the displacement corresponding to the peak sand shear strength. The shear stress of the sand-geogrid interface continues to increase, with a peak interface shear strength approaching the shear strength of the sand at comparatively large shear displacements.
 - The interface shear strength coefficient (α) for the sand-geogrid interfaces tested in this study ranges from 0.92 to 1.01. Conventional equations proposed to predict the sand-geogrid interface shear strength shows that the predicted values are smaller than the measured results.
 - The passive resistance contribution ratio (β) is proposed to quantify the passive resistance contribution in relation to the overall shear strength of sand-geogrid interfaces. The passive resistance contribution ratio averages 6.3% for the sand-geogrid interfaces tested in this study. These results indicate that the passive resistance is a relevant contribution under direct shear mode.
 - The passive resistance contribution ratio is positively correlated with the interface shear strength coefficient, the geogrid stiffness, and the tensile strength of longitudinal and transversal ribs, but it is negatively correlated with the aperture length and percent open area of the geogrid.
- This study provides evidence that the passive resistance be-

tween soil and geogrid interface is not negligible. A simple equation is proposed to evaluate the contribution of passive resistance to the overall shear strength of sand-geogrid interface under direct shear mode.

Notation

The following symbols are used in this paper:

- α = interface shear strength coefficient;
- β = passive resistance contribution ratio;
- δ = interface friction angle between sand to geosynthetic;
- μ_α = mean value of interface shear strength coefficient;
- μ_β = mean value of passive resistance contribution ratio;
- σ_n = normal stress;
- σ_α = standard deviation of interface shear strength coefficient;
- σ_β = standard deviation of passive resistance contribution ratio;
- ρ = percent open area;
- φ_{ds} = internal friction angle of sand;
- τ_{sand} = internal shear strength of sand;
- $\tau_{sand-geogrid}$ = shear strength of sand-geogrid interface; and
- $\tau_{sand-geotextile}$ = shear strengths of sand-geotextile interface.

References

- Abu-Farsakh, M. Y., and Coronel, J. (2006). "Characterization of cohesive soil-geosynthetic interaction from large direct shear test." *Proc., 85th Transportation Research Board Annual Meeting*, Washington, D.C.
- Alfaro, M. C., Miura, N., and Bergado, D. T. (1995). "Soil geogrid reinforcement interaction by pullout and direct shear tests." *Geotech. Test. J.*, 18(2), 157–167.
- ASTM. (2002). "Standard test method for determining the coefficient of soil and geosynthetic or geosynthetic and geosynthetic friction by the direct shear method." *D5321-02*, ASTM, West Conshohocken, Pa.
- Bakeer, R. M., Sayed, M., Cates, P., and Subramanian, R. (1998). "Pull-out and shear test on geogrid reinforced lightweight aggregate." *Geotext. Geomembr.*, 16(2), 119–133.
- Bauer, G. E., and Zhao, Y. (1993). "Evaluation of shear strength and dilatancy behavior of reinforced soil from direct shear tests." *ASTM Spec. Tech. Publ.*, 1190, 138–157.
- Bergado, D. T., Chai, J. C., Abiera, H. O., Alfaro, M. C., and Balasubramanian, A. S. (1993). "Interaction between cohesive-frictional soil and various grid reinforcements." *Geotext. Geomembr.*, 12(4), 327–349.
- Cancelli, A., Rimoldi, P., and Togni, S. (1992). "Frictional characteristics of geogrids by means of direct shear and pullout tests." *Proc., Int. Symp. on Earth Reinforcement Practice*, Kyushu Univ., Fukuoka, Japan, 51–56.
- Cazzuffi, D., Picarelli, L., Ricciuti, A., and Rimoldi, P. (1993). "Laboratory investigations on the shear strength of geogrid reinforced soils." *ASTM Spec. Tech. Publ.*, 1190, 119–137.
- Federal Highway Administration. (2001). "Performance test for geosynthetic reinforced soil including effects of preloading." *FHWA-RD-01-118*, Research, Development and Technology, Turner-Fairbank Highway Research Center, 270.
- Hatami, K., and Bathurst, R. J. (2006). "Numerical model for reinforced soil segmental walls under surcharge loading." *J. Geotech. Geoenviron. Eng.*, 132(6), 673–684.

- Jarret, P. M., and Bathurst, R. J. (1985). "Frictional development at a gravel geosynthetic peat interface." *Proc., 2nd Canadian Symp. of Geotextiles and Geomembranes*, Edmonton, Canada, 1–6.
- Jewell, R. A. (1990). "Reinforcement bond capacity." *Geotechnique*, 40(3), 513–518.
- Koerner, R. M., Wayne, M. H., and Carroll, R. G., Jr. (1989). "Analytic behavior of geogrid anchorage." *Proc., Geosynthetics'89 Conf*, IFAI, San Diego, 525–536.
- Lopez, M. L. (2002). "Soil geosynthetic interaction." *Geosynthetics and their applications*, Thomas Telford, London.
- Martin, J. P., Koerner, R. M., and Whitty, J. E. (1984). "Experimental friction evaluation of slippage between geomembranes, geotextiles, and soils." *Proc., Int. Conf. Geomembranes*, IFAI, St. Paul, Minn., 191–196.
- Milligan, G. W. E., Earl, R. F., and Bush, D. I. (1990). "Observations of photo-elastic pullout tests on geotextiles and geogrids." *Proc., 4th Int. Conf. on Geotextiles, Geomembranes and Related Products*, Vol. 2, Hague, The Netherlands, 747–751.
- Palmeira, E. M. (2004). "Bearing force mobilisation in pullout tests on geogrids." *Geotext. Geomembr.*, 22(6), 481–509.
- Palmeira, E. M., and Milligan, G. W. E. (1989). "Scale and other factors affecting the results of the pullout tests of grids buried in sand." *Geotechnique*, 39(4), 551–584.
- Sugimoto, M., Alagiyawanna, A. M. N., and Kadoguchi, K. (2001). "Influence of rigid and flexible face on geogrid pullout tests." *Geotext. Geomembr.*, 19(5), 257–328.
- Tatlisoz, N., Edil, T. B., and Benson, C. H. (1998). "Interaction between reinforcing geosynthetics and soil-tire chip mixtures." *J. Geotech. Geoenviron. Eng.*, 124(11), 1109–1119.
- Teixeira, S. H. C., Bueno, B. S., and Zornberg, J. G. (2007). "Pullout resistance of individual longitudinal and transverse geogrid ribs." *J. Geotech. Geoenviron. Eng.*, 133(1), 37–50.